

# Feasibility Study on Cryogenic Milling of Carbon Fiber Reinforced Silicon Carbide Composites

XU Liang<sup>1</sup>, ZHAO Guolong<sup>2\*</sup>, ZHANG Jianqiang<sup>2</sup>, WANG Kai<sup>1</sup>,  
WANG Xinyong<sup>1</sup>, HAO Xiuqing<sup>2</sup>

1. Aerospace Research Institute of Materials & Processing Technology, Science and Technology on Advanced Functional Composites Laboratory, Beijing 100076, P. R. China;
2. College of Mechanical and Electrical Engineering, Nanjing University of Aeronautics and Astronautics, Nanjing 210016, P. R. China

(Received 26 March 2020; revised 23 April 2020; accepted 18 May 2020)

**Abstract:** Carbon fiber reinforced silicon carbide matrix ( $C_f/SiC$ ) composites have the most potential application for high-temperature components of aerospace high-end equipment. However, high cutting temperature, rapid tool wear and severe surface damages are the main problems in dry cutting  $C_f/SiC$  composites process. The feasibility study on cryogenic milling of  $C_f/SiC$  composites using liquid nitrogen as coolant is investigated. Influences of milling parameters and coolant on temperature, cutting force, surface quality and tool wear are investigated, which is compared with dry cutting. Experimental results reveal that the cutting temperature in cryogenic milling of  $C_f/SiC$  composites is reduced by about 40%—60% compared with dry cutting. The milling force increases gradually with the increase of spindle speed, feed rate, depth and width of milling in cryogenic milling process. In addition, the machined surface quality in cryogenic milling is superior to that in dry cutting process. Fiber fracture, matrix damage and fiber matrix debonding are main material removal mechanisms. Flank face wear is the main wear form of the polycrystalline diamond (PCD) end mills. The tool life is prolonged in the cryogenic milling process because the reduced temperature inhibits the softening of Co binder and phase transition of diamond in the PCD end mills.

**Key words:**  $C_f/SiC$  composites; cryogenic milling; cutting temperature; surface quality; tool wear

**CLC number:** TH161

**Document code:** A

**Article ID:** 1005-1120(2020)03-0424-10

## 0 Introduction

Carbon fiber reinforced silicon carbide matrix ( $C_f/SiC$ ) composites have many superior mechanical and thermal properties, such as low density, high hardness, high specific strength, excellent wear resistance, high thermal stability, and chemical corrosion resistance. These properties make  $C_f/SiC$  composites widely used in thermal protection systems of space vehicle, nozzles and flaps of rocket motors, car brake systems, aero engine, et al.<sup>[1-3]</sup>. Generally, components made of  $C_f/SiC$  composites are manufactured in near-the-net shape. However,

the secondary machining process, address such as drilling, milling, and grinding, is still necessary in order to obtain the required dimensional tolerance and surface quality. The machinability of  $C_f/SiC$  composites is poor because of their high hardness and brittleness, as well as heterogeneous and anisotropic characteristics. The machining process is featured by rapid tool wear, low process efficiency, surface defects in terms of cavities, cracks, delamination and subsurface damage<sup>[4-7]</sup>.

Many studies have been conducted on the machining of  $C_f/SiC$  composites with traditional and non-traditional processes<sup>[8]</sup>. Among them, the grind-

\*Corresponding author, E-mail address: zhaogl@nuaa.edu.cn.

**How to cite this article:** XU Liang, ZHAO Guolong, ZHANG Jianqiang, et al. Feasibility study on cryogenic milling of carbon fiber reinforced silicon carbide composites[J]. Transactions of Nanjing University of Aeronautics and Astronautics, 2020, 37(3):424-433.

<http://dx.doi.org/10.16356/j.1005-1120.2020.03.009>

ing and the ultrasonic vibration assisted machining are widely used. The material removal mechanisms in grinding of  $C_f/SiC$  composites were studied via single-abrasive scratch tests<sup>[9-10]</sup>. The results showed that the grinding parameters had significant influence on the surface quality and subsurface defects. The grinding force decreased with increase of the grinding speed. The damage behaviors of the composites consisted of fiber breakage, fiber/matrix interfacial debonding and matrix cracking. Tawakoli et al.<sup>[11]</sup> developed a specially designed segmented grinding wheel to reduce the rubbing and plowing regimes in grinding of  $C_f/SiC$  composites. The specific grinding energy decreased consequently, and the experimental results showed that the grinding forces reduced significantly using the presented method. Qu et al.<sup>[12]</sup> carried out an experimental study on minimum quantity lubrication (MQL) in grinding of  $C_f/SiC$  composites. The grinding temperature reduced substantially because a large amount of heat was removed by water vapor. Excellent surface quality and low grinding force were also achieved in the MQL process. Theoretical and experimental studies have presented that ultrasonic vibration assisted machining can reduce the cutting force and obtain high surface integrity<sup>[13]</sup>. Li et al.<sup>[14]</sup> carried out conventional grinding and ultrasonic assisted grinding on  $C_f/SiC$  composites. The results showed that the surface roughness of  $C_f/SiC$  composites machined by ultrasonic assisted grinding was smaller than that of by conventional grinding, and ultrasonic assisted grinding process had less damage to mechanical properties of the materials. Even though the improved surface quality can be achieved via grinding process, the material removal rate is relatively low. In addition, ultrasonic generator and complex machining system are needed in ultrasonic vibration assisted machining, which makes it costly.

Cryogenic machining technology refers to a cutting technology that uses cold air, liquid nitrogen or liquid carbon dioxide and other cryogenic fluids to cool workpieces, cutting tools or cutting areas in the cutting process. At present, many researchers have conducted research on cryogenic machining technology. Bermingham et al.<sup>[15]</sup> used liquid nitrogen as the coolant in turning Ti-6Al-4V and found that the

tool life increased under certain cutting parameters and the chip shape was also improved at the same time. Manimaran et al.<sup>[16]</sup> used liquid nitrogen as the coolant to carry out cryogenic grinding experiments on AISI D3 steel. Compared with dry and wet cooling, the cryogenic cooling reduced the surface roughness evidently. Dhar et al.<sup>[17]</sup> studied the cryogenic turning of AISI 1040 and E4340C steel with carbide cutters and found a significant reduction in the tool wear rate and the surface roughness through the application of cryogenic cooling. Sadik et al.<sup>[18]</sup> used physical vapor deposition (PVD) coated tools to mill Ti-6Al-4V under liquid carbon dioxide cooling. It demonstrated that with increasing the flow rate of coolant, the tool life was improved. Yang<sup>[19]</sup> carried out comparative study on dry and cryogenic cutting of 316L stainless steel. Liquid nitrogen was used as the coolant. It was concluded that the cryogenic cutting could get the improved surface quality, the reduced tool wear and cutting force.

At present, the cryogenic machining process is mainly applied to machine typical difficult-to-machine metallic materials, such as high-temperature alloy, titanium alloy, and high-strength steels. Very few reports on cryogenic machining of  $C_f/SiC$  composites can be noted. In this paper, the feasibility study on cryogenic milling of  $C_f/SiC$  composites using liquid nitrogen as the coolant is carried out. Cutting temperature, cutting force, tool wear, and the machined surface quality under various cutting parameters are investigated. The material removal mechanisms and tool wear mechanisms are analyzed. For comparison, dry milling is also conducted under the same cutting parameters.

## 1 Experimental Setup

$C_f/SiC$  composites are used as the workpiece material in this paper. The surface morphology and schematic diagram of the structure are shown in Fig.1. The carbon fiber yarns include warp yarns, weft yarns, and Z yarns. Warp yarns are alternately woven up and down on weft yarns on each layer of plain weave fabrics, while Z yarns are perpendicular to the warp and weft layers. The properties of the composites are provided in Table 1.

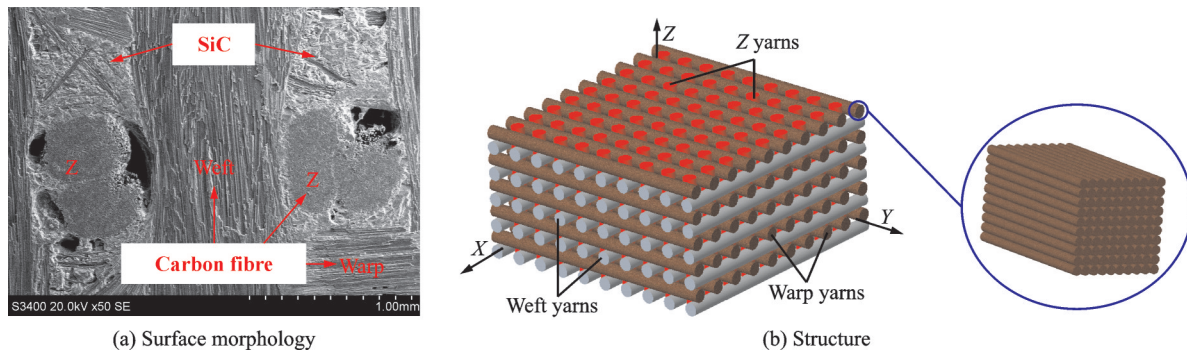


Fig.1 Surface morphology and structure of  $C_t/SiC$  composites

**Table 1** Material properties of  $C_t/SiC$  composites

Parameter	Value
Fiber volume /%	30
Porosity /%	15
Density /( $g \cdot cm^{-3}$ )	2.0
Tensile strength /MPa	200
Flexural strength /MPa	400
Young's modulus /GPa	40
Temperature resistance / $^{\circ}C$	1 500

The cryogenic milling experimental setup is shown in Fig. 2. The cryogenic cooling system includes a liquid nitrogen container, pressure gauges, valves, a stainless steel pipe covered with sponge, a nozzle with the inner diameter of 4 mm and some

clamping devices. The liquid nitrogen with a pressure of 1.1 MPa is sprayed into the cutting area. A five-axis machining center (MIKRON-UCP710) with a maximum spindle speed of 18 000 r/min and a maximum feed rate of 20 m/min is used. Down milling is adopted in all the experiments. The process parameters are listed in Table 2. Before each set of the experiment, the workpiece and the cutting tool are cooled for 5 min. Two fluted polycrystalline diamond (PCD) end mills are used. The diameter, the rake angle, the clearance angle and the inclination angle, of the end mill are 10 mm,  $3^{\circ}$ ,  $10^{\circ}$ , and  $0^{\circ}$ , respectively.

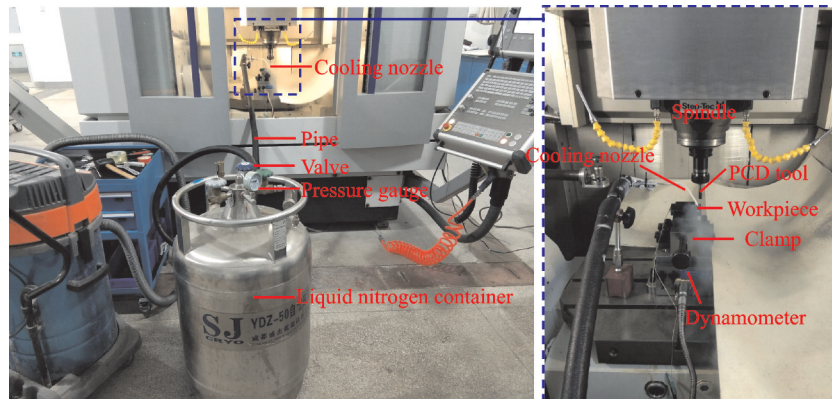


Fig.2 Experimental equipment of cryogenic cooling system and milling process

**Table 2** Machining parameters used in this work

Parameter	Value
Spindle speed $n / (r \cdot min^{-1})$	1 000, 3 000, 5 000, 7 000
Feed rate $v_f / (mm \cdot min^{-1})$	30, 60, 90, 120
Depth of milling $a_p / mm$	0.5, 1, 1.5, 2, 3
Width of milling $a_e / mm$	1, 2, 3, 4
Jet angle / ( $^{\circ}$ )	30, 60, 90
Coolant	Dry milling, liquid nitrogen

The schematic diagram of temperature measurement is shown in Fig. 3. A micro K-type thermo-

couple wire is sandwiched between two pieces of  $C_t/SiC$  blocks, and mica sheets are used to insulate them from each other. In the cutting process, thermocouple wires generate thermoelectric potential signals due to the change of the temperature. The signals are collected by a dynamic signal acquisition card (NI USB-6218), and then processed by the relevant software on the computer. The cutting force is measured with a dynamic dynamometer

(KISTLER 9625B). The surface morphology and microstructure of the material are observed by an optical microscope (VHX-600) and a scanning electron microscope (Hitachi S3400). The surface

roughness is measured by a laser scanning microscope (LSM 700). The tool wear morphology is observed by a digital camera microscope (UCMOS 10000KPA CCD).

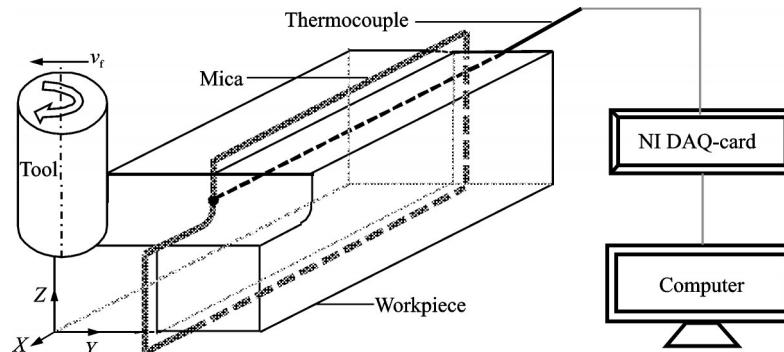


Fig.3 Illustration of cutting temperature measurement method

## 2 Results and Discussion

### 2.1 Cutting temperature

Fig.4 shows the milling temperature in both dry and cryogenic milling conditions when the spindle speed, feed rate, depth and width of milling are 3 000 r/min, 60 mm/min, 3 mm, and 2 mm, respectively. The temperature in cryogenic milling is 286–405 °C, while that in dry milling is about 732 °C. The temperature is significantly reduced by using liquid nitrogen as the coolant. This is because cryogenic liquid nitrogen can cool the cutting heat generated in the machining area, which can decrease the cutting temperature.

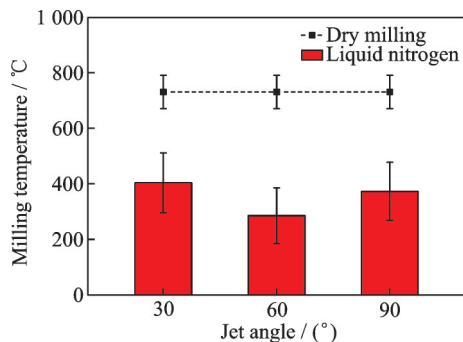


Fig.4 Milling temperature under different cooling conditions

In addition, the flowing liquid nitrogen has the functions of removing chips, lubricating the cutting area and reducing the heat generated by the friction

between the tool and the workpiece. Furthermore, the vaporization of liquid nitrogen can absorb a great quantity of cutting heat, taking away part of the heat from the tool, the workpiece and the cutting area. Therefore, the generated cutting temperature in cryogenic milling of  $C_f/SiC$  composites is significantly lower than that of in dry milling process.

### 2.2 Milling forces

Fig.5 shows the change of milling forces in three directions (cutting force  $F_x$ , thrust force  $F_y$  and axial cutting force  $F_z$ ) under different cutting parameters. It can be observed from Fig. 5 that  $F_y$  and  $F_z$  are far lower than  $F_x$  at the same cutting parameters. As shown in Fig.5(a), when the feed rate, the width and depth of milling are fixed, the cutting force of  $F_x$  increases with increase of the spindle speed. With the range of spindle speed increasing from 1 000 r/min to 5 000 r/min, the corresponding cutting force  $F_x$  increases dramatically. However, when the spindle speed increases from 5 000 r/min to 7 000 r/min, the increasing magnitude of  $F_x$  is relatively small. When the spindle speed, width and depth of milling are unchanged, milling forces in three directions show an increasing trend with an increment of feed rate (as shown in Fig.5(b)). When the feed rate increases, the nominal thickness and cross-sectional area of the cutting layer increase, the volume of the workpiece material that is cut in a unit

time increases, and then the extrusion, rebound and friction between the tool and the workpiece material constantly increase correspondingly. Therefore, the cutting resistance and the material deformation energy in the cutting process increase, resulting in an increase of the milling force with increasing the feed rate.

As shown in Fig.5(c), with increasing the width of milling from 1 mm to 4 mm,  $F_x$  increases continuously whereas the changes of  $F_y$  and  $F_z$  are relatively small. In addition, Fig.5(d) shows that

with increasing the depth of milling from 0.5 mm to 2 mm, the change of the cutting force  $F_x$  is extremely obvious and it is increased by a large margin. However, the milling forces in Y and Z directions is far lower than that in X direction, and the changing amplitude is also minor. As the depth or width of cutting increases, the geometry of the cutting layer changes and the area of the cutting layer increases, which promotes material removal rate, thereby increasing the friction between the tool and the cutting layer material and the cutting force.

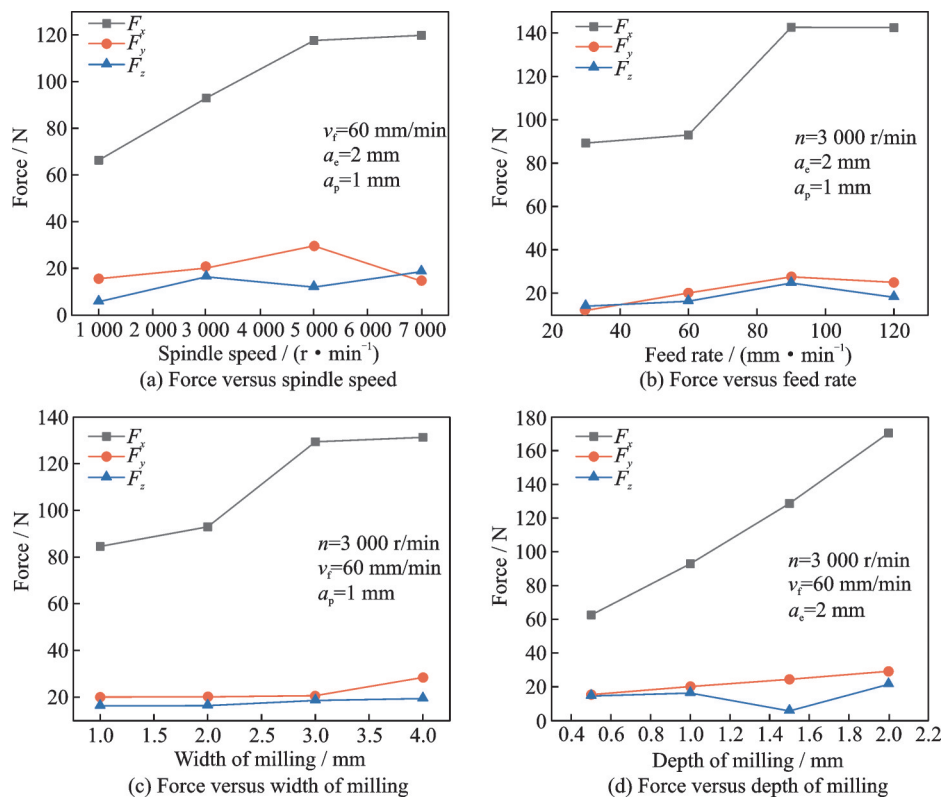


Fig.5 Variations of milling force in three directions under different cutting parameters

### 2.3 Surface quality and material removal mechanism

In this work, the processed surface of the  $C_f/SiC$  composites material is also composed of a SiC matrix between yarn, weft, Z carbon fiber yarn and carbon fiber, apart from the holes formed by the defects of the material itself. Fig.6 presents the removal process of carbon fiber yarn in three directions. Fig.7 shows the surface roughness of  $C_f/SiC$  composites processed under dry milling and cryogenic milling conditions at  $n=3000$  r/min,  $v_f=60$  mm/min,  $a_p=3$  mm and  $a_c=2$  mm. Under the cryogenic

ic milling condition, the surface roughness  $S_a$  and  $S_q$  of the machined surface area of warp, weft and Z yarns are significantly lower than those under dry milling condition. Thus, the surface quality in liquid nitrogen cooling assisted milling condition is better than that of in dry milling. The reason is that excellent cooling effect of liquid nitrogen can reduce the plasticity of the carbon fiber and deformation degree of the workpiece material in the cutting zone, thereby reducing the deformation of the machining surface and improving the quality of the machined surface.

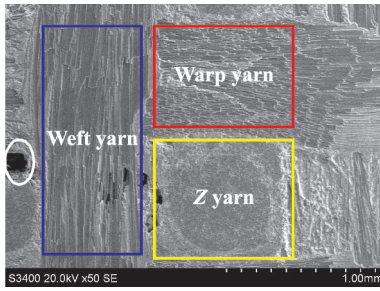


Fig.6 SEM image of the machined surface

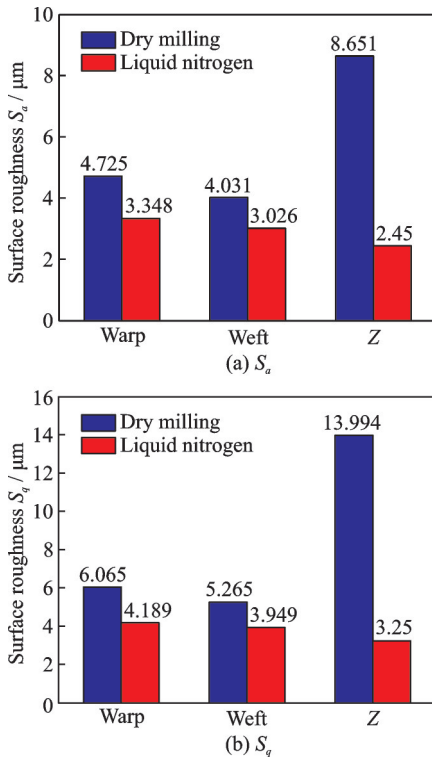


Fig.7 Surface roughness of the machined surface under dry and cryogenic milling conditions

Fig.8 presents the schematic diagram of material removal process while milling  $C_f/SiC$  composites along with the warp direction. Due to different mechanical properties, the removal mechanism of carbon fiber is different from that of the matrix material. SiC ceramic matrix is a typical brittle and difficult-to-cut material with high strength. During the cutting process, the silicon carbide material has little bending, tensile and compressive deformation. However, cracks continue to appear and propagate in the matrix, eventually leading to the failure of materials. Different from the silicon carbide, carbon fiber has relatively low strength, high toughness and plastic mechanical properties. Therefore, in the milling process, the carbon fiber in  $C_f/SiC$  composites

can bend and deform with limited deflection. In addition, carbon fibers are prone to brittle fracture under the effects of compressive stress, shear stress and bending stress.

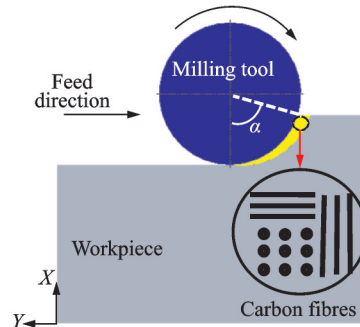


Fig.8 Schematic diagram of material removal process

As shown in Fig.9, this study divides carbon fibers in three fiber directions (warp, weft, Z) to discuss the material removal mechanism. The angle  $\alpha$  is defined as the rotation angle of the milling cutter in the stage of cutting into the workpiece. The angle  $\beta$  is defined as the counter-clockwise angle between the cutting speed direction and the carbon fiber direction. Fig.9(a) describes the schematic diagram of the removal mechanism of the warp carbon fiber yarn. In this case, the angle  $\beta$  is an obtuse angle. In addition, the shear force on the carbon fiber and the matrix is much higher than the compression force and the bending force. Under the action of stress, the inner of the carbon fiber and matrix have the occurrence of minor crack, which continues to extend until brittle fracture occurs (shown in the yellow rectangle in Fig.9(a)). Furthermore, the process of brittle fracture of carbon fiber by the shearing force also generates shearing and compressive forces on the surrounding fibers, which continues to generate long crack, eventually leading to brittle fracture.

In Fig.9(b), the compression and bending forces on the carbon fiber and the matrix are greater than the shear forces because the angle  $\beta$  is an acute angle. In addition, the matrix is brittle material and exist minor deformation under the stress, where carbon fiber has high bending strength and it will deform to a certain extent after being stressed, thereby

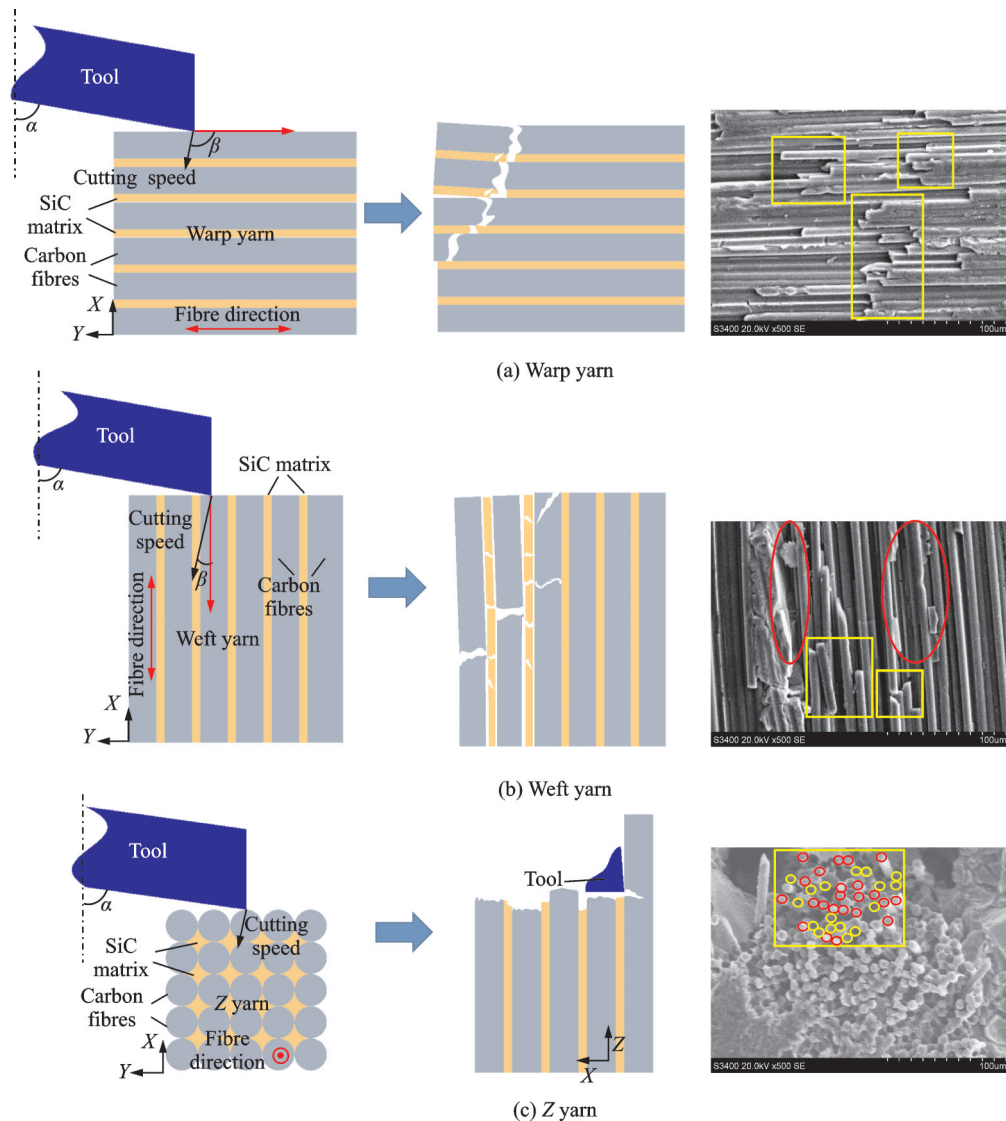


Fig.9 Illustrations of material removal process for warp , weft and Z yarns

leading to the debonding of the interface. Furthermore, carbon fiber is under the action of compressive and bending forces, and the stress concentration is mainly at the bottom. When the stress is greater than the breaking strength, brittle fracture occurs at the bottom of the carbon fiber. The brittle matrix collapses or fails due to the huge stresses that continue to generate the crack and extend to the entire area of  $C_f/SiC$  composites. The carbon fiber and substrate in the  $Z$  direction are mainly affected by the shearing force of the milling cutter bottom edge and the pressing force of the rake face. The carbon fiber and the matrix have the occurrence of brittle fracture along with the cutting direction under the action of shearing and compression forces, thereby achieving material removal. The material bonding

strength at the yarn crossings is low and more pitted. In addition, during the milling process, the carbon fiber is relatively easy to bend and deform after being stressed, and the crack occurs. After the fiber breaks from the bottom or the head, the carbon fiber pulls up along with the surface near the pit.

#### 2.4 Tool wear

In this work, tool wear under the milling parameters of  $n = 3\ 000$  r/min,  $v_t = 60$  mm/min,  $a_p = 3$  mm and  $a_e = 2$  mm is studied. The main failure of polycrystalline diamond (PCD) tool is flank face wear. The wear area of tool flank face is characterized with a digital camera microscope, and the width of wear land  $VB$  is measured. The value of wear criteria in this paper is  $VB = 0.3$  mm. Fig.10 shows the width of flank face wear  $VB$  under dry

milling and cryogenic milling of  $C_t/SiC$  composites. It can be observed that with the increase of the milling length, the width of flank face wear increases rapidly and the tool wear is faster in the initial stage, while later  $VB$  increases slowly. However, the changes of  $VB$  on the flank face under two conditions are obviously different. Compared with the cryogenic milling, the overall growth rate of  $VB$  during the dry milling is higher, that is, the tool wear in the dry milling is faster than that in the cryogenic milling. In the cryogenic milling, the increase of  $VB$  is relatively slow and  $VB$  reaches the wear criteria until the milling length attaining 4 000 mm. The tool durability is improved by the cryogenic milling compared with the dry cutting.

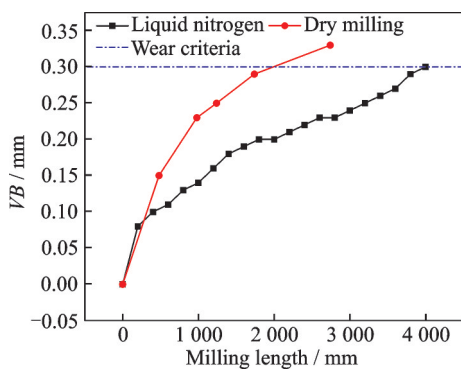


Fig.10 Width of flank wear land

In addition, in the process of liquid nitrogen assisted milling of  $C_t/SiC$  composites, the liquid nitrogen medium can suppress the tool wear and prolong the tool service life. Furthermore, due to the cooling effect of liquid nitrogen, the cutting temperature reduces, thus avoiding the tool material phase transition, the binder softening and adhesive wear on the tool during liquid nitrogen assisted milling process.

Fig.11 shows the tool wear morphology of the flank face. In the dry milling experiments, the wear of tool flank face is stepped and the wear land is relatively uniform, resulting in the breakage of the cutting edge and tool nose. This is due to the high milling temperature during the dry milling, which causes the softening of the tool binder Co phase, resulting in a decrease in the bonding strength of the tool material, a reduction in the strength of the cutting edge, and the failure of the cutting tool. With

the friction and scratch of chips between the workpiece and the cutting tool, and the tool material phase transition caused by high temperature, the tool wear rate aggravates rapidly. During the process of the cryogenic milling, continuous high-frequency scratches and serious frictional shocks take place on the cutting tool, resulting in obvious groove-like wear on the cutting edge and the side zone. Owing to the cooling effect of liquid nitrogen, the cutting temperature remains lower than both of the phase transition temperature of the tool material and the softening temperature of the binder. Therefore, no obvious adhesive wear is observed.

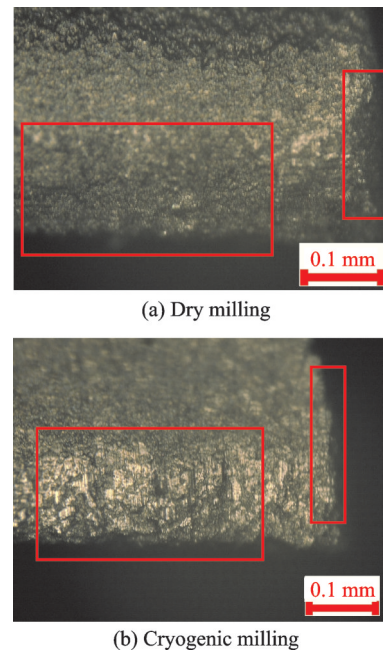


Fig.11 Morphologies of tool flank face wear under two conditions

### 3 Conclusions

The feasibility study on the cryogenic milling of  $C_t/SiC$  composites using liquid nitrogen as the coolant is carried out. Under the same cutting parameters, the cutting temperature generated by the cryogenic milling is extremely lower than that in the dry cutting of  $C_t/SiC$  composites. In addition, thrust force  $F_y$  and axial force  $F_z$  are obviously lower than cutting force  $F_x$  at the same cutting parameters, and cutting force  $F_x$  increases gradually with one of these parameters including spindle speed, feed rate, depth and width of milling in the process

of cryogenic milling with the aid of liquid nitrogen. Fiber fracture, matrix damage and fiber matrix debonding are main material removal mechanisms during the cutting process. Furthermore, the surface roughness  $S_a$  and  $S_q$  of the machined surface area of warp, weft and  $Z$  yarns in cryogenic milling are significantly lower than that in dry cutting at  $n = 3\ 000$  r/min,  $v_f = 60$  mm/min,  $a_p = 3$  mm, and  $a_e = 2$  mm. The main wear mechanism of PCD tool in cryogenic milling is flank face wear, and the wear rate is slower than that in dry cutting process.

### References

- [1] WEI C J, ZHAO L, HU D J, et al. Electrical discharge machining of ceramic matrix composites with ceramic fiber reinforcements[J]. *The International Journal of Advanced Manufacturing Technology*, 2013, 64(1/2/3/4): 187-194.
- [2] NASLAIN R. Design preparation and properties of non-oxide CMCs for application in engines and nuclear reactors: An overview[J]. *Composites Science & Technology*, 2004, 64(2): 155-170.
- [3] BAO Y J, BI M Z, GAO H, et al. Effect of fiber directions on the surface quality of milling  $C_f/SiC$  composites[J]. *Advanced Materials Research*, 2013, 797: 196-201.
- [4] LI Z C, JIAO Y, DEINES T W, et al. Rotary ultrasonic machining of ceramic matrix composites: Feasibility study and designed experiments[J]. *International Journal of Machine Tools & Manufacture*, 2005, 45(12/13): 1402-1411.
- [5] LIU Y S, WANG C H, LI W N, et al. Effect of energy density on the machining character of C/SiC composites by picosecond laser[J]. *Applied Physics*, 2014, A116(3): 1221-1228.
- [6] SHAN Y C, HE N, LI L, et al. Entrance and exit defects during coarse pitch orbital drilling of carbon fiber reinforced plastic plates[J]. *Transactions of Nanjing University of Aeronautics & Astronautics*, 2016, 33(6): 696-705.
- [7] ZHANG L, HU J, TIAN W, et al. Critical thrust force forecasting for drilling exit delamination of carbon fibre reinforced plastics[J]. *Transactions of Nanjing University of Aeronautics & Astronautics*, 2017, 34(4): 372-379.
- [8] HU M, MING W W, AN Q L, et al. Experimental study on milling performance of 2D C/SiC composites using polycrystalline diamond tools[J]. *Ceramics International*, 2019, 45(8): 10581-10588.
- [9] LI Y C, GE X, WANG H, et al. Study of material removal mechanisms in grinding of C/SiC composites via single-abrasive scratch tests[J]. *Ceramics International*, 2019, 45(4): 4729-4738.
- [10] LIU Q, HUANG G Q, CUI C C, et al. Investigation of grinding mechanism of a 2D  $C_f/C-SiC$  composite by single-grain scratching[J]. *Ceramics International*, 2019, 45(10): 13422-13430.
- [11] TAWAKOLI T, AZARHOUSHANG B. Intermittent grinding of ceramic matrix composites (CMCs) utilizing a developed segmented wheel[J]. *International Journal of Machine Tools & Manufacture*, 2011, 51(2): 112-119.
- [12] QU S S, GONG Y D, YANG Y Y, et al. Investigating minimum quantity lubrication in unidirectional  $C_f/SiC$  composite grinding[J]. *Ceramics International*, 2020, 46(3): 3582-3591.
- [13] CHEN J, MING W W, AN Q L, et al. Mechanism and feasibility of ultrasonic-assisted milling to improve the machined surface quality of 2D  $C_f/SiC$  composites [J]. *Ceramics International*, 2020. DOI: <https://doi.org/10.1016/j.ceramint.2020.03.047>.
- [14] LI X D, ZHAO Y M, ZHANG X F, et al. Influence of machining process parameters on property of C/SiC composites[J]. *Aerospace Materials & Technology*, 2015, 45(4): 104-107.
- [15] BERMINGHAM M J, KIRSCH J, SUN S, et al. New observations on tool life, cutting forces and chip morphology in cryogenic machining of Ti-6Al-4V [J]. *International Journal of Machine Tools & Manufacture* 2011, 51(6): 500-511.
- [16] MANIMARAN G, PRADEEP K M, VENKATASAMY R. Surface modifications in grinding AISI D3 steel using cryogenic cooling[J]. *Journal of the Brazilian Society of Mechanical Sciences and Engineering*, 2015, 37(4): 1357-1363.
- [17] DHAR N R, PAUL S, CHATTOPADHYAY A B. The influence of cryogenic cooling on tool wear, dimensional accuracy and face finish in turning AISI 1040 and E4340C steels[J]. *Wear*, 2001, 249(10/11): 932-942.
- [18] SADIK M I, ISAKSON S, MALAKIZADI A, et al. Influence of coolant flow rate on tool life and wear development in cryogenic and wet milling of Ti-6Al-4V [J]. *Procedia CIRP*, 2016, 46: 91-94.
- [19] YANG Weiliang. Study on cooling cutting of 316L stainless steel[D]. Taiyuan: Taiyuan University of Science and Technology, 2010. (in Chinese)

**Acknowledgements** This work was supported by the Na-

tional Natural Science Foundation of China (Nos. 51705249, 51875285), the China Postdoctoral Science Foundation (No. 2019M661823), the Aeronautical Science Foundation of China (No. 2017ZE52047), and the Defense Industrial Technology Development Program (No. JCKY2018605C018). The authors realize that the time and space available for a review of such an ambitious subject are limited and, thus, regretfully, we are unable to cover many important contributions. The authors would like to acknowledge the following people for their assistance: HE Ning, LI Liang, HE Lei, XIA Hongjun, and HU Maoshun, all with the College of Mechanical and Electrical Engineering, NUAA.

**Authors** Dr. XU Liang received his B.S. and Ph.D. degrees of Mechanical Engineering from Shandong University in 2007 and 2013, respectively. His research has focused on high performance machining of composite materials, development of ultra-hard cutting tools, high precision and low defect machining of difficult-to-cut materials.

Dr. ZHAO Guolong received his B.S. and Ph.D. degrees of Mechanical Engineering from Shandong University in 2009 and 2015, respectively. Now he is an associate professor of College of Mechanical and Electrical Engineering in Nanjing University of Aeronautics and Astronautics (NUAA). His research interests include advanced cutting technology, high performance cutting of composite materials, micro machining and micro-tool technology.

**Author contributions** Dr. XU Liang conducted the analysis, interpreted the results, and checked the manuscript. Dr. ZHAO Guolong designed the study, and designed the experimental setup. Mr. ZHANG Jianqiang conducted the experiments and wrote the manuscript. Dr. WANG Kai analyzed the tool wear mechanisms. Dr. WANG Xinyong analyzed the surface morphology. Dr. HAO Xiuqing contributed to the discussion and background of the study. All authors commented on the manuscript draft and approved the submission.

**Competing interests** The authors declare no competing interests.

(Production Editor: WANG Jing)

## 碳纤维增强碳化硅基复合材料的低温铣削研究

徐亮<sup>1</sup>, 赵国龙<sup>2</sup>, 张健强<sup>2</sup>, 王凯<sup>1</sup>, 王新永<sup>1</sup>, 郝秀清<sup>2</sup>

(1. 航天材料及工艺研究所先进功能复合材料技术重点实验室, 北京 100076, 中国;

2. 南京航空航天大学机电学院, 南京 210016, 中国)

**摘要:**碳纤维增强碳化硅基复合材料(C<sub>f</sub>/SiC复合材料)是航空航天高端装备热端构建最具潜力的新型高温结构材料,但是其干切削存在切削温度高、刀具磨损快和加工损伤严重等问题。本文研究了C<sub>f</sub>/SiC复合材料的液氮低温铣削特性,并开展了低温切削和干切削的对比试验研究。阐明了铣削用量和低温介质对切削温度、切削力、加工表面质量和刀具磨损的影响规律。结果表明,液氮低温铣削C<sub>f</sub>/SiC复合材料的切削温度比干切削降低了40%—60%;低温铣削中,随着铣削用量的增加,切削力逐渐升高;低温铣削的加工表面质量优于干切削。C<sub>f</sub>/SiC复合材料的去除机理主要包括纤维断裂、基体破坏和纤维与基体脱黏等。PCD铣刀的主要失效形式是后刀面磨损,液氮低温铣削中低温阻碍了PCD铣刀中粘结剂Co软化和金刚石相变,因此刀具寿命得到提高。

**关键词:**C<sub>f</sub>/SiC复合材料;低温铣削;切削温度;表面质量;刀具磨损